11th International Conference on Ground Penetrating Radar, June 19-22, 2006, Columbus Ohio, USA

GPR without a source

Evert Slob, Deyan Draganov and Kees Wapenaar
Department of Geotechnology, Delft University of Technology
Mijnbouwstraat 120, 2628 RX, Delft, The Netherlands
e.c.slob@tudelft.nl

***Abstract*— Using passive radar is known in radiometry and for localization of electromagnetic field sources. These sometimes rely on interferometric principles. Here we present a study that uses a different concept of interferometry. With interferometry we mean the creation of data from autocorrelation or crosscorrelation of two recorded data traces without the use of active sources. The sources must then have other, unknown, origins. The obtained result is as if the transmitter was located at one of the passive receiver locations, while the receiver was located at the other passive receiver location. Under favorable conditions, the original sources play no role in the final result. The exact mathematical formulation of this principle is based on time reversal invariance, which can be represented as an interaction quantity for reciprocity theorems. We derive here representations for the Green's function for the electric field due to electric current sources. To arrive at representations that can be used in practice, some approximations must be made. We discuss and illustrate the effects of the approximations and of non-zero medium conductivities.**

***Index Terms*— interferometry, data creation, crosscorrelation, time reversal, passive GPR.**

I. INTRODUCTION

Passive radar techniques have a long history. Usually they are used for localization of electromagnetic fields [1], or for radiometry applications, e.g., for Earth observation [2]. In this paper we extend the use of interferometric techniques and adopt the notion of interferometry introduced by Schuster [3] to include the creation of new data. This idea dates back to 1968 when Claerbout [4] showed that the autocorrelation of an acoustic plane wave transmission response recorded in a one-dimensional configuration at the pressure-free surface yields the reflection response at the pressure-free surface. Weaver and Lobkis showed that the autocorrelation function of an acoustic wavefield response is the wavefield response of a direct pulse-echo experiment in a three-dimensional configuration [5]. The condition is that the wavefield is diffuse, which in their case was generated by thermal noise. Based on the diffusivity of the wavefield, many authors showed similar results also for crosscorrelations in open and closed configurations [6], [7], [8]. Later it was shown for deterministic instantaneously reacting media that Claerbout's principle could be extended to three-dimensional media [9], [10].

Here we use the reaction principles set out by Bojarski [11] as the basis for our derivations and derive new interferometric representations for the electric field Green's function for an electric current source. The configuration is a bounded domain with a closed surface at which sources are active. Inside this bounded domain two receivers are present that record all responses from the sources located on the boundary. When these two recordings are crosscorrelated, the result is independent of the location of the closed boundary and independent of the sources. It represents the field as if it was generated at one of the two recording locations and received at the other location together with its time-reversed version. When one receiver is inside the domain and the other is outside the domain a similar result is obtained but now only the causal field is constructed. These representations are only valid for instanteneously reacting media, since time-reversal invariance relies on the conservation of total wave energy. We show that the concept can still be used when the conduction losses are limited to values where radar wave methods are effective.

II. LOCAL TIME-REVERSAL INVARIANCE

In our paper we use the subscript notation for vectors and tensors, Einstein's summation convention applies to repeated lower case Latin subscripts to which the values 1, 2 and 3 are to be assigned. We use the electric field vector $\hat{\boldsymbol{E}}(\boldsymbol{x},\omega)$, the magnetic field vector $\hat{\boldsymbol{H}}(\boldsymbol{x},\omega)$, and the external source volume densities of electric and magnetic currents, $\{\hat{\boldsymbol{J}}^e(\boldsymbol{x},\omega),\hat{\boldsymbol{J}}^m(\boldsymbol{x},\omega)\}$, respectively. The medium parameters are electric permittivity $\varepsilon_{kr}(\boldsymbol{x})$, electric conductivity $\hat{\sigma}^e_{kr}(\boldsymbol{x},\omega)$, magnetic permeability $\mu_{jp}(\boldsymbol{x})$ and the magnetic conductivity $\hat{\sigma}^m_{jp}(\boldsymbol{x},\omega)$. Note that we have defined the electric permittivity and the magnetic permeability as functions of position only. This is no restriction because the time dependence of these medium parameters can be incorporated in the electric and magnetic conductivities, respectively.

We define the time-Fourier transform of a space-time dependent quantity as

$$\hat{\boldsymbol{E}}(\boldsymbol{x},\omega)=\int_{t=0}^{\infty}\exp(-\mathrm{j}\omega t)\boldsymbol{E}(\boldsymbol{x},t)\mathrm{d}t, \tag{1}$$

where j is the imaginary unit and ω denotes angular frequency.

In the space-frequency domain Maxwell's equations in matter are given by

$$-\epsilon_{kmj}\partial_m\hat{H}_j+[\hat{\sigma}^e_{kr}+\mathrm{j}\omega\varepsilon_{kr}]\hat{E}_r=-\hat{J}^e_k, \tag{2}$$

$$\epsilon_{jmr}\partial_m\hat{E}_r+[\hat{\sigma}^m_{jp}+\mathrm{j}\omega\mu_{jp}]\hat{H}_p=-\hat{J}^m_j, \tag{3}$$

where ∂_m denotes partial differentiation with respect to the coordinate x_m and ϵ_{kmj} is the anti-symmetric tensor of rank three, $\epsilon_{kmj}=1$ when $kmj=\{123,231,312\}$, $\epsilon_{kmj}=-1$ when $kmj=\{132,213,321\}$, while $\epsilon_{kmj}=0$ otherwise.

For the time-correlation type reciprocity theorem we need the complex conjugate of Maxwell's equations

$$-\epsilon_{kmj}\partial_m\hat{H}^*_j + [\hat{\sigma}^{e*}_{kr} - \mathrm{j}\omega\varepsilon_{kr}]\hat{E}^*_r = -\hat{J}^{e*}_k, \quad (4)$$

$$\epsilon_{jmr}\partial_m\hat{E}^*_r + [\hat{\sigma}^{m*}_{jp} - \mathrm{j}\omega\mu_{jp}]\hat{H}^*_p = -\hat{J}^{m*}_j, \quad (5)$$

where the asterisk denotes complex conjugation. The corresponding interaction quantity is given by

$$\partial_m\epsilon_{mkj}\left(\hat{E}^*_{k,A}\hat{H}_{j,B} + \hat{E}_{k,B}\hat{H}^*_{j,A}\right), \quad (6)$$

upon taking state A as the time-reversed state. For reciprocal media, which implies that the medium parameters in the two states are the same,

$$\varepsilon_{kr,A}(\boldsymbol{x}) = \varepsilon_{rk,B}(\boldsymbol{x}), \qquad \hat{\sigma}^e_{kr,A}(\boldsymbol{x},\omega) = \hat{\sigma}^e_{rk,B}(\boldsymbol{x},\omega), \quad (7)$$

$$\mu_{jp,A}(\boldsymbol{x}) = \mu_{pj,B}(\boldsymbol{x}), \qquad \hat{\sigma}^m_{jp,A}(\boldsymbol{x},\omega) = \hat{\sigma}^m_{pj,B}(\boldsymbol{x},\omega). \quad (8)$$

The local electromagnetic reciprocity theorem of the time-correlation type is obtained by substituting both Maxwell's equations (2) and (3), for state B and the time-reversed Maxwell's equations (4) and (5), for state A into the interaction quantity of equation (6). For reciprocal media this results in

$$\begin{aligned}-\partial_m\epsilon_{mkj}\left(\hat{E}^*_{k,A}\hat{H}_{j,B} + \hat{E}_{k,B}\hat{H}^*_{j,A}\right)\\ = 2\hat{H}^*_{j,A}\Re\{\hat{\sigma}^m_{jp}\}\hat{H}_{p,B} + 2\hat{E}^*_{k,A}\Re\{\hat{\sigma}^e_{kr}\}\hat{E}_{r,B}\\ +\hat{J}^{e*}_{r,A}\hat{E}_{r,B} + \hat{J}^e_{r,B}\hat{E}^*_{r,A} + \hat{J}^{m*}_{p,A}\hat{H}_{p,B} + \hat{J}^m_{p,B}\hat{H}^*_{p,A}, \quad (9)\end{aligned}$$

where $\Re\{\hat{F}\}$ denotes real part of $\hat{F}$. In the following sections we apply this local reciprocity theorem to a bounded domain.

III. INTERFEROMETRIC GREEN'S FUNCTION REPRESENTATIONS

We start with the global form of the reciprocity theorem of the time-correlation type for the situation applied to the domain $\mathbb{D}$ with closed boundary $\partial\mathbb{D}$, which has a unique outward pointing unit normal n_m. Without loss of generality in the relaxation mechanisms, we have assumed that they are all contained in the electric and magnetic conductivity functions. We have assumed reciprocal media and the heterogeneities are not restricted to occur only inside the domain $\mathbb{D}$, but may extend over the whole space. Hence, we find an integral reciprocity theorem by integrating equation (9) over the domain $\mathbb{D}$ and applying Gauss' divergence theorem to the integral containing the interaction quantity. This leads to

$$\begin{aligned}\oint_{\boldsymbol{x}\in\partial\mathbb{D}} n_m\epsilon_{mkj}(\hat{E}^*_{k,A}\hat{H}_{j,B} + \hat{E}_{k,B}\hat{H}^*_{j,A})\mathrm{d}^2\boldsymbol{x}\\ = -2\int_{\boldsymbol{x}\in\mathbb{D}}[\hat{H}^*_{j,A}\Re\{\hat{\sigma}^m_{jp}\}\hat{H}_{p,B} + \hat{E}^*_{k,A}\Re\{\hat{\sigma}^e_{kr}\}\hat{E}_{r,B}]\mathrm{d}^3\boldsymbol{x}\\ -\int_{\boldsymbol{x}\in\mathbb{D}}\Big[(\hat{J}^e_{r,A})^*\hat{E}_{r,B} + \hat{J}^e_{k,B}\hat{E}^*_{k,A}\\ +\hat{J}^m_{j,B}\hat{H}^*_{j,A} + (\hat{J}^m_{p,A})^*\hat{H}_{p,B}\Big]\mathrm{d}^3\boldsymbol{x}. \quad (10)\end{aligned}$$

Equation (10) is the global reciprocity theorem of the time-correlation type as only products of quantities and complex conjugate quantities occur, which leads to correlations of these quantities in the time domain. For a more detailed discussion on reciprocity relations, see [12].

Normally we use electric-field receivers and sources and hence in equation (10) we take zero magnetic current sources and write the magnetic field vector in terms of the electric field vector in equation (10). Further we assume an instantaneous reacting medium and with constant scalar magnetic permeability in the neighborhood of the boundary, $\partial\mathbb{D}$, of the domain, $\mathbb{D}$. Substituting all these choices in equation (10) leads to

$$\begin{aligned}\frac{1}{\mathrm{j}\omega\mu}\oint_{\boldsymbol{x}\in\partial\mathbb{D}} n_m\epsilon_{mkj}\Big(\hat{E}^*_{k,A}(\epsilon_{jnr}\partial_n\hat{E}_{r,B})\\ -\hat{E}_{k,B}(\epsilon_{jnr}\partial_n\hat{E}^*_{r,A})\Big)\mathrm{d}^2\boldsymbol{x}\\ = \int_{\boldsymbol{x}\in\mathbb{D}}\Big[(\hat{J}^e_{r,A})^*\hat{E}_{r,B} + \hat{J}^e_{k,B}\hat{E}^*_{k,A}\Big]\mathrm{d}^3\boldsymbol{x}. \quad (11)\end{aligned}$$

The electric current source terms in the right-hand side of equation (11) are used to localize the receivers at $\boldsymbol{x}_A$ and $\boldsymbol{x}_B$. By assuming now also isotropy and homogeneity for the electric permittivity in the neighborhood of the closed boundary surface, $\partial\mathbb{D}$, it can be shown that the left-hand side can be rewritten in terms of time correlations of the electric field and normal derivatives of the electric field. This results in

$$\begin{aligned}\frac{1}{\mathrm{j}\omega\mu}\oint_{\boldsymbol{x}\in\partial\mathbb{D}}\Big(\hat{E}^*_{k,A}n_m\partial_m\hat{E}_{k,B} - \hat{E}_{r,B}n_m\partial_m\hat{E}^*_{r,A}\Big)\mathrm{d}^2\boldsymbol{x}\\ = \int_{\boldsymbol{x}\in\mathbb{D}}\Big[(\hat{J}^e_{r,A})^*\hat{E}_{r,B} + \hat{J}^e_{k,B}\hat{E}^*_{k,A}\Big]\mathrm{d}^3\boldsymbol{x}. \quad (12)\end{aligned}$$

3.1 Observation Points $\boldsymbol{x}_A$ and $\boldsymbol{x}_B$ Inside Domain $\mathbb{D}$

We define the observation points in this configuration in terms of impulsive sources with arbitrary orientations and their locations in the two states with $\{\boldsymbol{x}_A, \boldsymbol{x}_B\} \in \mathbb{D}$. Hence, the sources and the fields are given by,

$$\hat{J}_{k,A} = \delta_{kr}\delta(\boldsymbol{x} - \boldsymbol{x}_A); \hat{E}_{k,A} = \hat{G}_{kr}(\boldsymbol{x}, \boldsymbol{x}_A, \omega), \quad (13)$$

$$\hat{J}_{r,B} = \delta_{rs}\delta(\boldsymbol{x} - \boldsymbol{x}_B); \hat{E}_{r,B} = \hat{G}_{rs}(\boldsymbol{x}, \boldsymbol{x}_B, \omega). \quad (14)$$

Substituting equations (13) and (14) in equation (12) leads to

$$\begin{aligned}2\Re\{\hat{G}_{kr}(\boldsymbol{x}_A, \boldsymbol{x}_B, \omega)\} = -\frac{1}{\mathrm{j}\omega\mu}\\ \times\oint_{\boldsymbol{x}\in\partial\mathbb{D}}\Big(\{\hat{G}_{kj}(\boldsymbol{x}_A, \boldsymbol{x}, \omega)\}^* n_m\partial_m\{\hat{G}_{rj}(\boldsymbol{x}_B, \boldsymbol{x}, \omega)\}\\ -\{n_m\partial_m\hat{G}_{kp}(\boldsymbol{x}_A, \boldsymbol{x}, \omega)\}^*\{\hat{G}_{rp}(\boldsymbol{x}_B, \boldsymbol{x}, \omega)\}\Big)\mathrm{d}^2\boldsymbol{x}, \quad (15)\end{aligned}$$

where μ is the magnetic permeability of the medium in the neighborhood of the boundaryand where field reciprocity has been used to interchange the source and receiver positions in the argument of the green's functions. This is an exact representation for the real part of the electric field Green's function for an electric current source in terms of crosscorrelations of point source responses observed at $\boldsymbol{x}_A$ and $\boldsymbol{x}_B$ inside the domain $\mathbb{D}$. This is true for any heterogeneous anisotropic medium that is homogeneous and isotropic only in the neighborhood of the boundary $\partial\mathbb{D}$. To have a representation for the real part only is sufficient as it represents a causal function in the time domain together with its time-reversed version,

which do not overlap except at $t = 0$. This implies that in the frequency domain the imaginary part can be constructed from the real part via a Hilbert transformation. The two terms under the integral of equation (15) ensure that, when summed over all sources on the boundary, waves propagating outward from the sources at $\boldsymbol{x}$ on $\partial\mathbb{D}$ do not interact with those propagating inward and vice versa.

To bring equation (15) to a form that is more suited for practical applications we perform several manipulations, for which it is illustrative to split the Green's functions into terms denoting the waves propagating inward or outward from the sources on $\partial\mathbb{D}$,

$$\hat{G}_{kj;A} = \hat{G}^{(in)}_{kj;A} + \hat{G}^{(out)}_{kj;A}, \tag{16}$$

$$\hat{G}_{rj;B} = \hat{G}^{(in)}_{rj;B} + \hat{G}^{(out)}_{rj;B}, \tag{17}$$

where the superscripts (in) and (out) denote the inward and outward propagating waves and we have written the Green's functions $\hat{G}_{kj}(\boldsymbol{x}_A, \boldsymbol{x}, \omega)$ and $\hat{G}_{rj}(\boldsymbol{x}_B, \boldsymbol{x}, \omega)$ as $\hat{G}_{kj;A}$ and $\hat{G}_{rj;B}$. In the high-frequency regime, the main contributions to the integral in equation (15) come from stationary points on the boundary [13], [14], [15]. At those points the absolute cosines of the ray angles for $\hat{G}_{kj;A}$ and $\hat{G}_{rj;B}$ are the same. This implies for example that the terms $\hat{G}^{(in)*}_{kj;A}\partial_m\hat{G}^{(in)}_{rj;B}$ and $-\hat{G}^{(in)}_{rj;B}\partial_m\hat{G}^{(in)*}_{kj;A}$ give the same contribution to the integral, whereas the contributions of $\hat{G}^{(in)*}_{kj;A}\partial_m\hat{G}^{(out)}_{rj;B}$ and $-\hat{G}^{(out)}_{rj;B}\partial_m\hat{G}^{(in)*}_{kj;A}$ cancel each other. We use this to rewrite equation (15) as

$$2\Re\{\hat{G}_{kr}(\boldsymbol{x}_A, \boldsymbol{x}_B, \omega)\} = -\frac{2}{\mathrm{j}\omega\mu} \times \oint_{\boldsymbol{x}\in\partial\mathbb{D}} \left(\hat{G}^{(in)*}_{kj;A}\partial_m\hat{G}^{(in)}_{rj;B} + \hat{G}^{(out)*}_{kj;A}\partial_m\hat{G}^{(out)}_{rj;B}\right) n_m \mathrm{d}^2\boldsymbol{x}. \tag{18}$$

To measure the inward and outward propagating waves separately is impossible without source decomposition methods, which requires full control over the sources. Assuming we do not have that, we use equations (16) and (17) to write equation (18) as

$$2\Re\{\hat{G}_{kr}(\boldsymbol{x}_A, \boldsymbol{x}_B, \omega)\} + \text{'ghost'} = -\frac{2}{\mathrm{j}\omega\mu} \times \oint_{\boldsymbol{x}\in\partial\mathbb{D}} \{\hat{G}_{kj}(\boldsymbol{x}_A, \boldsymbol{x}, \omega)\}^* n_m\partial_m\{\hat{G}_{rj}(\boldsymbol{x}_B, \boldsymbol{x}, \omega)\}\mathrm{d}^2\boldsymbol{x}, \tag{19}$$

where the 'ghost' is given by,

$$\text{'ghost'} = -\frac{2}{\mathrm{j}\omega\mu} \times \oint_{\boldsymbol{x}\in\partial\mathbb{D}} \left(\hat{G}^{(in)*}_{kj;A}\partial_m\hat{G}^{(out)}_{rj;B} + \hat{G}^{(out)*}_{kj;A}\partial_m\hat{G}^{(in)}_{rj;B}\right) n_m \mathrm{d}^2\boldsymbol{x}. \tag{20}$$

The right-hand side of equation (19) contains only a single product of crosscorrelations and is therefor a more manegable form than equation (15). Unfortunately, in equation (19) a ghost-term is present that leads to spurious events in the reconstructed Green's function $\hat{G}_{kr}(\boldsymbol{x}_A, \boldsymbol{x}_B, \omega)$. These spurious event are non-physical contributions and, unlike the physical events, they depend on the source locations. This means that when the boundary is irregularly shaped the contributions are not integrated coherently and can lead to a zero contribution, depending on the distribution of the sources. In such cases the ghost-contribution can be ignored and equation (19) can be used to construct the Green's function, which was first numerically demonstrated by [16].

We extend our assumption of a homogeneous and isotropic medium to exist also outside the domain $\mathbb{D}$. Waves that leave the domain $\mathbb{D}$ never enter it again, implying that the boundary is convex seen from the inside of $\mathbb{D}$. Then the outward propagating waves are never recorded, hence, equation (20) vanishes and we find,

$$2\Re\{\hat{G}_{kr}(\boldsymbol{x}_A, \boldsymbol{x}_B, \omega)\} = -\frac{2}{\mathrm{j}\omega\mu} \times \oint_{\boldsymbol{x}\in\partial\mathbb{D}} \{\hat{G}_{kj}(\boldsymbol{x}_A, \boldsymbol{x}, \omega)\}^* n_m\partial_m\{\hat{G}_{rj}(\boldsymbol{x}_B, \boldsymbol{x}, \omega)\}\mathrm{d}^2\boldsymbol{x}, \tag{21}$$

where now μ is the magnetic permeability of the whole embedding. Finally, if we take the boundary $\partial\mathbb{D}$ to be a sphere with large enough radius such that the Fraunhofer far-field conditions apply [17], we can approximate the normal derivative as $-\mathrm{j}\frac{\omega}{c}|\cos(\alpha(\boldsymbol{x}))|$, where we only need a minus sign because only ingoing waves contribute to the final result and $\alpha(\boldsymbol{x})$ denotes the angle of emission a generalized ray makes with the unit normal on $\partial\mathbb{D}$. Assuming $\alpha(\boldsymbol{x}) = 0$ for all source locations, we obtain

$$2\Re\{\hat{G}_{kr}(\boldsymbol{x}_A, \boldsymbol{x}_B, \omega)\} \approx -\frac{2}{\mu c} \times \oint_{\boldsymbol{x}\in\partial\mathbb{D}} \{\hat{G}_{kj}(\boldsymbol{x}_A, \boldsymbol{x}, \omega)\}^* \{\hat{G}_{rj}(\boldsymbol{x}_B, \boldsymbol{x}, \omega)\}\mathrm{d}^2\boldsymbol{x}, \tag{22}$$

where $c = (\varepsilon\mu)^{-1/2}$ is the electromagnetic wave velocity in the embedding. Equations (15)-(22) are the electromagnetic equivalents of the acoustic and elastic representations for open configurations given in [18]. Each integrand in the right-hand side of equation (22) is an electric field generated by an impulsive souce of arbitrary direction and located at position $\boldsymbol{x}$ on the boundary and the k-component is recorded at location $\boldsymbol{x}_A$, while the r-component is recorded at location $\boldsymbol{x}_B$. By crosscorrelating these two recordings in the time domain and then summing over all source directions at all locations on the boundary yields the real part of the k-component electric field Green's function recorded at $\boldsymbol{x}_A$ and generated by the r-component of an impulsive source at location $\boldsymbol{x}_B$. This representation only involves the electric-field electric-current-source Green's function and can be used for efficient modeling schemes. An acoustic example of this idea can be found in [19]. If the radius of the sphere is taken large enough, the error involved can be made arbitrarily small and hence the approximation sign does not involve a large error. The accuracy depends very much on the total contribution from waves that leave the boundary in other than the normal direction. For generalized rays with increasing angle of emission, relative to the the normal vector of the boundary, progressively larger errors are involved with making the far-field approximation. These errors are therefore depending on

the location of the source on the boundary. This is a potential cause of spurious events because waves that should cancel when summed over all sources will now not show complete destructive interference. In general we can state that amplitude errors that depend on the source location on the boundary can lead to spurious events. In principle this is serious because there is no way to identify spurious from physical events when they occur in the time window of interest.

3.2 Observation Point $\boldsymbol{x}_A$ Inside $\mathbb{D}$, while $\boldsymbol{x}_B$ Outside $\mathbb{D}$

We define the observation points in this configuration in terms of impulsive sources with arbitrary orientations and their locations in the two states with $\boldsymbol{x}_A \in \mathbb{D}$, while $\boldsymbol{x}_B \notin \mathbb{D}$. We hence define the sources and the fields as,

$$\hat{J}_{k,A} = \delta_{kr}\delta(\boldsymbol{x}-\boldsymbol{x}_A); \hat{E}_{k,A} = \hat{G}_{kr}(\boldsymbol{x},\boldsymbol{x}_A,\omega), \quad (23)$$

$$\hat{J}_{r,B} = \delta_{rs}\delta(\boldsymbol{x}-\boldsymbol{x}_B); \hat{E}_{r,B} = \hat{G}_{rs}(\boldsymbol{x},\boldsymbol{x}_B,\omega). \quad (24)$$

Substituting equations (23) and (24) in equation (12) leads to

$$\hat{G}_{kr}(\boldsymbol{x}_A,\boldsymbol{x}_B,\omega) = -\frac{1}{\mathrm{j}\omega\mu} \times \oint_{\boldsymbol{x}\in\partial\mathbb{D}} \Big(\{\hat{G}_{kj}(\boldsymbol{x}_A,\boldsymbol{x},\omega)\}^* n_m \partial_m \{\hat{G}_{rj}(\boldsymbol{x}_B,\boldsymbol{x},\omega)\} - \{n_m\partial_m \hat{G}_{kp}(\boldsymbol{x}_A,\boldsymbol{x},\omega)\}^* \{\hat{G}_{rp}(\boldsymbol{x}_B,\boldsymbol{x},\omega)\} \Big) \mathrm{d}^2\boldsymbol{x}. \quad (25)$$

This is an exact representation for the total electric field Green's function for an electric current source in terms of crosscorrelations of point source responses observed at $\boldsymbol{x}_A$ and $\boldsymbol{x}_B$ inside the domain $\mathbb{D}$. This is true for any heterogeneous anisotropic medium that is homogeneous and isotropic only in the neighborhood of the boundary $\partial\mathbb{D}$. This implies that the exact causal Green's function is obtained. Notice that the right-hand side of equation (25) looks similar to the right-hand side of equation (15), but while the Green's function for location $\boldsymbol{x}_A$ is indeed the same, the Green's function for $\boldsymbol{x}_B$ is very different. The two terms under the integral of equation (15) ensure that waves propagating outward from the sources at $\boldsymbol{x}$ on $\partial\mathbb{D}$ do not interact with those propagating inward and vice versa. In this new configuration, waves that travel from $\boldsymbol{x}$ to $\boldsymbol{x}_A$ and whose travel time is larger than for waves that travel from the same source at $\boldsymbol{x}$ to $\boldsymbol{x}_B$ arrive at negative times. When summed over all sources for which this applies, these waves must exactly cancel each other. Waves for which the total travel time from a source location $\boldsymbol{x}$ to the receiver location at $\boldsymbol{x}_A$ is smaller than from the same source to receiver location $\boldsymbol{x}_B$ arrive at possitive times. Summing over all these waves leads to the exact causal Green's function as if there were an impulsive electric current source in $\boldsymbol{x}_B$ and the electric field were recorded at $\boldsymbol{x}_A$. Also for this configuration we would like to arrive at representations that can be used in practice. We extend again our assumption of a homogeneous and isotropic medium to exist also outside the domain $\mathbb{D}$. Waves that leave the domain $\mathbb{D}$ never enter it again, implying that the boundary is convex seen from the inside of $\mathbb{D}$. It can then be shown by a similar stationary phase analysis as given in [13], [14] that the terms under the integral are approximately equal but with opposite sign for waves that initially travel toward $\mathbb{D}$ from the sources on the boundary, as in the situation when both observation points are inside $\mathbb{D}$. However, in this new configuration the receiver location $\boldsymbol{x}_B$ is located outside $\mathbb{D}$ and waves that travel initially outward from the sources on the boundary are recorded at $\boldsymbol{x}_B$ and correlated with waves that are ingoing waves and recorded at $\boldsymbol{x}_A$. For these waves the two terms are approximately equal and with the same sign when summed over all sources on the boundary. Since we cannot decompose the wave fields at the sources in terms of ingoing and outgoing waves, we make the assumption that is correct for initially ingoing waves and neglect the error for interactions with waves that travel initially outward and recorded at $\boldsymbol{x}_B$ and hence, we obtain,

$$\hat{G}_{kr}(\boldsymbol{x}_A,\boldsymbol{x}_B,\omega) + \text{'ghost'} = -\frac{2}{\mathrm{j}\omega\mu} \times \oint_{\boldsymbol{x}\in\partial\mathbb{D}} \{\hat{G}_{kj}(\boldsymbol{x}_A,\boldsymbol{x},\omega)\}^* n_m \partial_m \{\hat{G}_{rj}(\boldsymbol{x}_B,\boldsymbol{x},\omega)\} \mathrm{d}^2\boldsymbol{x}, \quad (26)$$

where the 'ghost' is given by,

$$\text{'ghost'} = -\frac{2}{\mathrm{j}\omega\mu} \oint_{\boldsymbol{x}\in\partial\mathbb{D}} \left(\hat{G}^{(in)*}_{kj;A} \partial_m \hat{G}^{(out)}_{rj;B} \right) n_m \mathrm{d}^2\boldsymbol{x}. \quad (27)$$

In this configuration the ghost term is non-zero even when the embedding is homogeneous. The presence of the ghost term leads to large errors in the retrieved Green's function because ingoing waves recorded at $\boldsymbol{x}_A$ are correlated with outgoing waves recorded at $\boldsymbol{x}_B$ and these should have been canceled. Of course, the travel time from the sources on the boundary to the receiver at $\boldsymbol{x}_A$ is subtracted from the travel time from the sources on the boundary directly to $\boldsymbol{x}_B$. If we are able to have the receiver at $\boldsymbol{x}_B$, in terms of travel time, closer to the boundary than $\boldsymbol{x}_A$, we ensure that all spurious events arrive before the first desired arrival and most arrive at negative times. Since we only construct the causal Green's functions, events arriving at negative times are directly identified as spurious events and hence present no problem for interferometric use. Finally, if we take the boundary $\partial\mathbb{D}$ to be a sphere with large enough radius such that the Fraunhofer far-field conditions apply, we obtain

$$\hat{G}_{kr}(\boldsymbol{x}_A,\boldsymbol{x}_B,\omega) \approx -\frac{2}{\mu c} \times \oint_{\boldsymbol{x}\in\partial\mathbb{D}} \{\hat{G}_{kj}(\boldsymbol{x}_A,\boldsymbol{x},\omega)\}^* \{\hat{G}_{rj}(\boldsymbol{x}_B,\boldsymbol{x},\omega)\} \mathrm{d}^2\boldsymbol{x}. \quad (28)$$

Each integrand in the right-hand side of equation (28) is an electric field generated by an impulsive souce of arbitrary direction and located at position $\boldsymbol{x}$ on the boundary and the k-component is recorded at location $\boldsymbol{x}_A$, while the r-component is recorded at location $\boldsymbol{x}_B$. By crosscorrelating these two recordings in the time domain and then summing over all source locations on the boundary yields the k-component electric field Green's function recorded at $\boldsymbol{x}_A$ and generated by the r-component of an impulsive source at location $\boldsymbol{x}_B$. The radius of the sphere cannot be taken arbitrarily large and the error involved cannot be made arbitrarily small. The accuracy

depends very much on the total contribution from waves that leave the boundary in other than the normal direction. The above arguments for generating spurious events in the configuration with both receivers located inside $\mathbb{D}$ also apply here.

IV. TRANSIENT SOURCES

In situations where we have control over the sources, such as in the laboratory, we can modify equation (22) to incorporate the time signatures of the sources. To this end we define electric wavefield recordings at the receiver locations $\boldsymbol{x}_A$ and $\boldsymbol{x}_B$ as

$$\hat{E}^{\rm obs}_{kj}(\boldsymbol{x}_A,\boldsymbol{x},\omega) = \hat{G}^{EJ^e}_{kj}(\boldsymbol{x}_A,\boldsymbol{x},\omega)\hat{s}^{(j)}(\boldsymbol{x},\omega), \quad (29)$$

$$\hat{E}^{\rm obs}_{kj}(\boldsymbol{x}_B,\boldsymbol{x},\omega) = \hat{G}^{EJ^e}_{kj}(\boldsymbol{x}_B,\boldsymbol{x},\omega)\hat{s}^{(j)}(\boldsymbol{x},\omega), \quad (30)$$

where $\hat{s}^{(j)}(\boldsymbol{x})$ denotes the source frequency spectrum in the x_j-direction at position $\boldsymbol{x}$, which can be different for each direction and for each source position. The power spectrum of the sources is defined as

$$\hat{S}^{(j)}(\boldsymbol{x},\omega) = \hat{s}^{(j)*}(\boldsymbol{x},\omega)\hat{s}^{(j)}(\boldsymbol{x},\omega). \quad (31)$$

We further introduce a shaping filter, $\hat{F}^{(j)}(\boldsymbol{x},\omega)$, under the assumption that we know the source frequency spectrum at all locations as

$$\hat{F}^{(j)}(\boldsymbol{x},\omega) = \frac{Y\hat{S}_0(\omega)}{\hat{S}^{(j)}(\boldsymbol{x},\omega)}, \quad (32)$$

where $Y = 1/(\mu c)$ denotes the plane wave admittance of the embedding and $\hat{S}_0$ is the desired source power spectrum. This choice allows a different source signature for each source direction and for each source position along the boundaries and we can still have a single source power spectrum, $\hat{S}_0$, in the corrrelation result.

4.1 Observation Points $\boldsymbol{x}_A$ and $\boldsymbol{x}_B$ Inside Domain $\mathbb{D}$

Using the definitions of equations (29)-(32) in equation (22) we find

$$\Re\{\hat{G}^{EJ^e}_{kr}(\boldsymbol{x}_A,\boldsymbol{x}_B,\omega)\}\hat{S}_0 \approx -\oint_{\boldsymbol{x}\in\partial\mathbb{D}} \hat{F}^{(j)}(\boldsymbol{x},\omega)\{\hat{E}^{\rm obs}_{kj}(\boldsymbol{x}_A,\boldsymbol{x},\omega)\}^*\{\hat{E}^{\rm obs}_{rj}(\boldsymbol{x}_B,\boldsymbol{x},\omega)\}{\rm d}^2\boldsymbol{x} \quad (33)$$

when both $\boldsymbol{x}_A \in \mathbb{D}$ and $\boldsymbol{x}_B \in \mathbb{D}$. This expression can be used in practical applications when all sources are excited separated in time such that for each source position a full recording can be made. These can be natural sources as long as the above requirement of independent measurements is fulfilled. In this way we obtain independent measurements each of which can be plotted to form a so-called correlation gather, which, under favorable conditions, also allows for the identification of spurious events in case of conductive media or due to the far-field approximation.

4.2 Observation Point $\boldsymbol{x}_A$ Inside $\mathbb{D}$, while $\boldsymbol{x}_B$ Outside $\mathbb{D}$

Using the definitions of equations (29)-(32) in equation (28) we find

$$\hat{G}^{EJ^e}_{kr}(\boldsymbol{x}_A,\boldsymbol{x}_B,\omega)\hat{S}_0 + \text{ 'ghost'} \approx -2\oint_{\boldsymbol{x}\in\partial\mathbb{D}} \hat{F}^{(j)}(\boldsymbol{x},\omega)\{\hat{E}^{\rm obs}_{kj}(\boldsymbol{x}_A,\boldsymbol{x},\omega)\}^*\{\hat{E}^{\rm obs}_{rj}(\boldsymbol{x}_B,\boldsymbol{x},\omega)\}{\rm d}^2\boldsymbol{x}, \quad (34)$$

when $\boldsymbol{x}_A \in \mathbb{D}$, while $\boldsymbol{x}_B \notin \mathbb{D}$. The ghost term is equivalent to equation (ghostio) but now includes the shaping filter. This expression can be used in practical applications when all sources are excited separated in time such that for each source position a full recording can be made. These can be natural sources as long as the above requirement of independent measurements is fulfilled. In this way we obtain independent measurements each of which can be plotted to form a so-called correlation gather, which, under favorable conditions, also allows for the identification of spurious events in case of conductive media or due to the far-field approximation. In case we can design the configuration such that all travel times of outward traveling waves from the boundary to the observation point at $\boldsymbol{x}_B$ are smaller than those of the inward traveling waves from the boundary to the receiver station at $\boldsymbol{x}_A$, all events of the ghost arrive at negativve times and present no problem.

V. NUMERICAL RESULTS

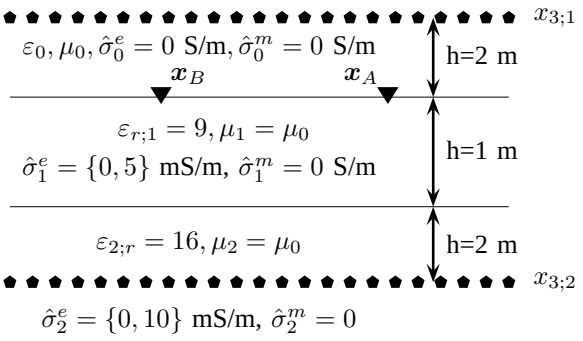

Fig. 1. Configuration for the 2D examples, with a three layer medium and with zero and non-zero values for the electric conductivity to investigate the effects of conductivity in crosscorrelation interferometry methods.

We show numerical results to illustrate the concept, the effect of the far-field approximation and the effect of presence of conduction losses in the medium, which is often encountered in GPR applications. For the second configuration with one receiver outside the domain enclosed by the sources, we also illustrate the effect of introducing spurious events due to the erroneous handling the interaction between ingoing waves recorded $\boldsymbol{x}_A$ and outgoing waves recorded at $\boldsymbol{x}_B$. All theory above is derived for three dimensions, but all examples are from a two-dimensional model consisting of a plane layered earth. In that case the closed boundary is opened and extended to infinity on the sides, which leads to zero contributions from the sides [20]. The top layer is the upper half space as a model for air, with free space electromagnetic parameters, the second layer has a thickness of 1 m, a velocity of 10 cm/ns and in

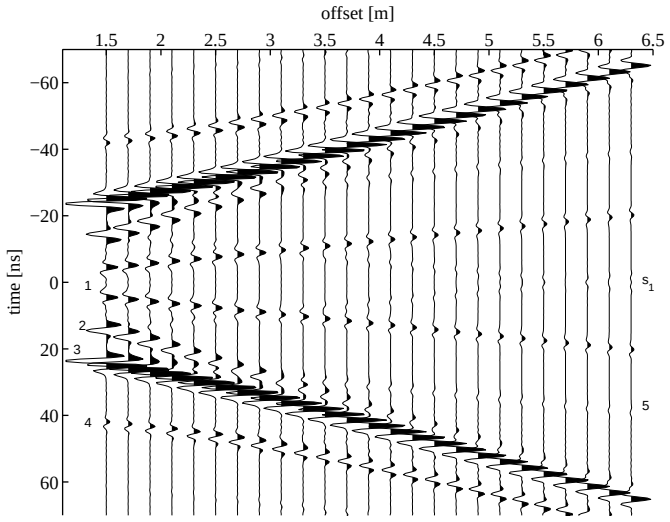

Fig. 2. CMP constructed from using the far field approximation in the crosscorrelation of several antennas, initial offset is 1.5 m and with 20 cm stepsize. The events are labeled as the direct airwave (1), direct ground wave (2), primary reflection at the interface (3), first order multiple reflection between surface and interface (4), refraction at the surface from the primary reflection at large enough offsets (5) and the spurious event (s_1).

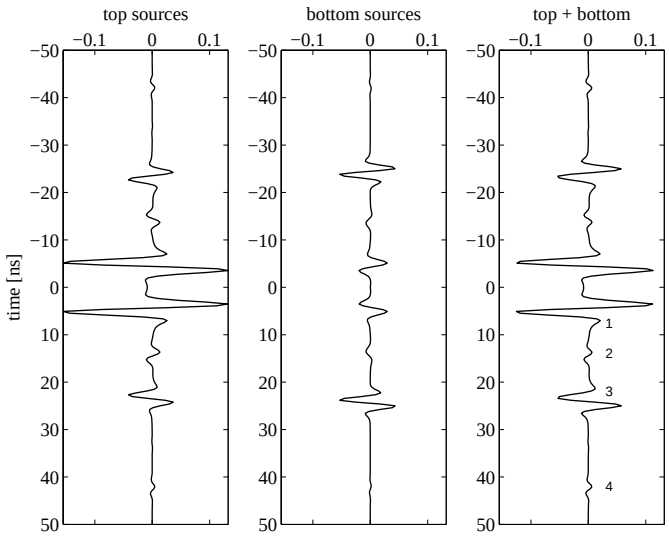

Fig. 3. Contributions from the sources at the top and bottom surfaces in a conductive medium to the crosscorrelation results compared to the directly modeled result at an antenna offset of 1.5 m.

case we study the effects of conduction losses a conductivity of 5 mS/m, while the the third layer is the lower half space with a velocity of 7.5 cm/ns and in case we study the effects of conduction losses a conductivity of 10 mS/m, see Figure 1. If we study the effects of the approximations, all layers are assumed non-conductive. At the end we show an example of the combined effects. The sources in the upper half space are, at $x_{3;1}$, 2 m above the earth surface, while the sources in the lower half space are, at $x_{3;2}$, 2 m below the second interface. In the configuration where both receivers are located inside $\mathbb{D}$ then they are at the surface in the air as a model for the usual surface reflection GPR survey with two parallel antennas. This reduces all representations to the two-dimensional TE-mode configuration. As argued in the previous section, the far-field approximation can lead to spurious events. Resulting spurious events are the consequence of incomplete destructive interference due to source location dependent amplitude errors. This is demonstrated to be actual in Figure 2, where a CMP gather is shown, obtained using the far-field approximation of equation (22). The numbered events in the figure are the direct air- and ground waves (labeled 1 and 2), the primary reflection from the interface between the layer and the lower half space (labeled 3) and the first order multiple reflection between the top and bottom interfaces of the layer. The CMP gather looks fine at first sight, but a small amplitude spurious event springs off (labeled s_1 in the graph) from the small offset causal direct groundwave and its arrival time decreases with increasing offset. This event also occurs in a time-symmetric form. The amplitude of the spurious event is, in this example, very small.

To study the effect of conduction losses we have introduced non-zero conductivity values in the first layer, $\sigma = 5$ mS/m, and the lower half space, $\sigma = 10$ mS/m. The high-frequency limit of the intrinsic attenuation for the two layers is

$$\text{ATT} = 816 \times \sigma/\sqrt{\varepsilon_r} \text{ dB/m}. \tag{35}$$

Hence, the attenuation is ATT=-2.04 dB/m for the lower half space and ATT=-1.4 dB/m for the layer. From these numbers we see that the amplitude is halved every 1.5 m and 2.2 m of propagation distance in the lower half space and in the layer, respectively. These are attenuation values that fall well within the range where GPR can be used. All events coming from the bottom source boundary have been most dramatically influenced by the conduction loss factor in the lower half space, which is clearly seen in Figure 3 where we observe that the contribution from sources on the bottom boundary is relatively small. The direct ground wave is almost absent. The contributions to the primary reflection from the sources on the top and bottom boundaries are slightly out of phase due to the conduction losses, which can be seen from the fact that their sum in the right plot has almost the same maximum amplitude as the seperate events in the left and middle plots. From Figure 4 the directly modeled result is shown together with the causal part of the crosscorrelation result to show that the amplitude of the reflection is an order of magnitude smaller than it should be. Here we see that the direct airwave has the wrong amplitude. In Figure 5 we show a close up of the first order reflection where the crosscorrelation result has been multiplied with a factor 13 to emphasize the phase difference compared to the exact arrival. The onset of the reflection in the crosscorrelation result is clearly advanced while it is correct toward the end of the reflection event. The event has become more distorted due to the construction from events that have traveled over a larger distance in the layer than required for the

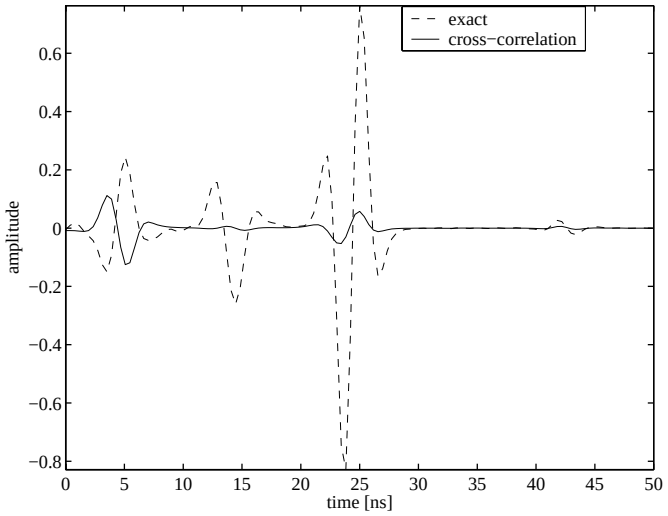

Fig. 4. Comparison of crosscorrelation result in a conductive medium with the directly modeled result of the conductive model at an antenna offset of 1.5 m.

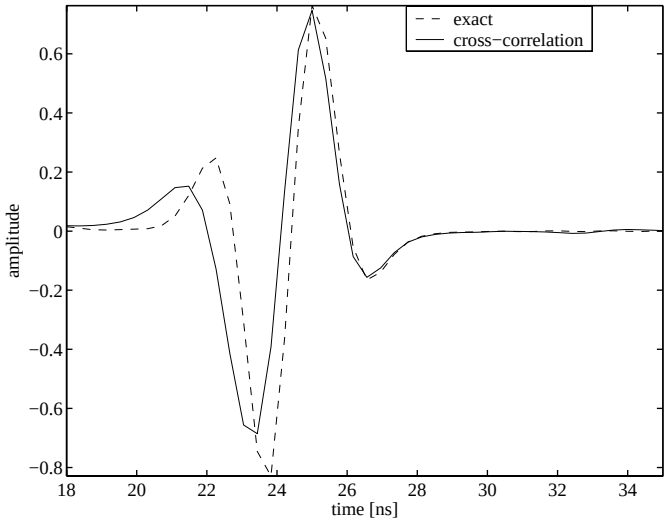

Fig. 5. Close up of the reflection event of Figure 4 with the amplitude of the crosscorrelation result blown up by a factor 13.

reflection event itself and for contributions from sources in the lower half space more dispersion is introduced because waves contributing to the final reflection event have also traveled in the lower half space. Combining errors due to conduction losses and due to the dipole-to-monopole approximation shows that no extra effects occur. This can be seen by comparing it to the result of the far-field approximated solution for the model with zero conductivities given in Figure 2 with Figure 6, where the CMP gather is plotted for the approximate solution with non-zero conductivities in the subsurface layers. Of course, due to the conduction losses all amplitudes have decreased, but four of the five expected events are visible, be it with some errors in arrival time and in amplitude, and only the direct ground wave is missing and replaced by a single spurious event (s_1) that is easily identifiable because its arrival time

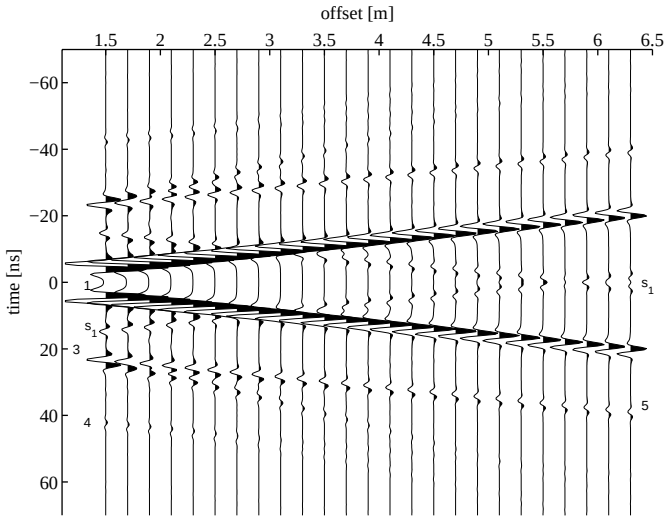

Fig. 6. CMP constructed from using the dipole-tomonopole approximation in the crosscorrelation of several antennas, initial offset is 1.5 m and with 20 cm stepsize, in conductive layered earth.

decreases with increasing offsets. From this we corroborate our conclusion in the previous section that amplitude errors that depend on the source location on the boundary surface lead to slight phase and amplitude errors in desired reflection events and possibly to spurious events. Here we see that the presence of non-zero conductivities lead to similar effects, hence the effects occur irrespective of the origin of the amplitude errors in the individual source contributions. Amplitude errors in the desired events due to the dipole-to-monopole approximation are small compared to errors due to conduction losses. Still, this type of radar wave interferometry can be used in GPR applications where medium to low loss factors are present. The kinematics of all events are almost correctly retrieved, for which reason we regard equation (33) suitable for radar wave interferometry.

VI. CONCLUSIONS

We have derived new interferometric representations for the electric field Green's function of an electric current source in two configurations. In the first configuration the two observation points are inside the bounded domain enclosed by a boundary containign sources. Crosscorrelation of the recordings at the two locations yields the Green's function as if there was a source present at one location, while it was recorded at the other location. The causal Green's function together with its time-reversed version is obtained with this representation. In the other configuration one of the recording locations is inside the bounded domain, while the other is outside. Here a similar result is obtained but now only the causal green's function is retrieved. The necessary modification to the exact repreentation in the second configuration leads to spurious events. A proper choice of the two recording locations allows moving all spurious events to arrive before the first desired event, which is known. Hence all spurious events are easily identified. The presence of non-zero conductivities introduces

errors of two kinds. The retrieved amplitudes of desired events are too small and due to position dependent amplitude errors for the sources on the boundary, spurious events are introduced due to incomplete destructive interference. This latter error is a similar cause for spurious events as due to the far field approximations and hence no new spurious events are introduced compared to the far field approximation. There we conclude that both configurations allow for the necessary modifications to arrive a practical representations, which lead to kinematically correct radargrams. For this reason we regard these representations as suitable for GPR interferometry and interferometric imaging purposes.

ACKNOWLEDGMENTS

This work is part of the research program of the Netherlands research center for Integrated Solid Earth Science (ISES). The research of DD is supported by the Dutch Technology Foundation STW under project number DET4915.

REFERENCES

[1] Knapp, C.H. and G.C. Carter, The generalized correlation method for estimating of time delay, *IEEE Trans. on Acoust., Speech, Signal Processing*, *24*, 320-327 (1976).

[2] Ruf, C. S., C. T. Swift, A. B. Tanner, and D. M. Le Vine, Interferometric synthetic aperture microwave radiometry for the remote sensing of the Earth, *IEEE Trans. Geosci. Remote Sensing*, *26*, 597-611 (1988).

[3] Schuster, G. , Theory of daylight/interferometric imaging: tutorial, *Extended Abstracts*, 63rd Mtg., Eur. Assoc. Geosc. & Eng., Paper: A32 (2001).

[4] Claerbout, J., Synthesis of a layered medium from its acoustic transmission response, *Geophysics*, *33*, 264–269 (1968).

[5] Weaver, R., and O. Lobkis, Ultrasonics without a source: Thermal fluctuation correlations at MHz frequencies, *Phys. Rev. Lett.*, *87*, 134301–1–4, doi:10.1103/PhysRevLett.87.134301 (2001).

[6] Lobkis, O., and R. Weaver, On the emergence of the Green's function in the correlations of a diffuse field, *JASA*, *110*, 3011–3017 (2001).

[7] Campillo, M., and A. Paul, Longe-range correlations in the diffuse seismic coda waves, *Science*, *299*, 547–549 (2003).

[8] van Tiggelen, B., Green function retrieval and time reversal in a disordered world, *Phys. Rev. Lett.*, *91*, 243904–1–4, doi:10.1103/PhysRevLett.91.243904 (2003).

[9] Wapenaar, C., D. Draganov, J. Thorbecke, and J. Fokkema, Theory of acoustic daylight imaging revisited, *Expanded Abstracts*, 72nd Annual Internat. Mtg. Soc. Expl. Geophys., 2269–2272 (2002).

[10] Derode, A., E. Larose, M. Tanter, J. de Rosny, A. Tourin, M. Campilo, and M. Fink, Recovering the Green's function from field-field correlations in an open scattering medium(L), *JASA*, *113*, no. 6, 2973–2976, doi:10.1121/1.1570436 (2003).

[11] Bojarski, N., Generalized reaction principles and reciprocity theorems for the wave equations, and the relationships between time-advanced and time-retarded fields., *JASA*, *74*, 281–285 (1983).

[12] de Hoop, A., *Handbook of radiation and scattering of waves*, Academic Press, Amsterdam (1995).

[13] Schuster, G. T., Yu, J., Sheng, J., and Rickett, J., Interferometric/daylight seismic imaging, *Geoph. J. Int.*, *157*, 838-852 (2004).

[14] Snieder, R., Extracting the Green's function from the correlation of coda waves: A derivation based on stationary phase, *Phys. Rev. E*, *69*, 046610–1–8, doi:10.1103/PhysRevE.69.046610 (2004).

[15] Wapenaar, K., D. Draganov, J. van der Neut, and J. Thorbecke, Seismic interferometry: a comparison of ap- proaches, *Expanded Abstracts*, 74th Annual Internat. Mtg., Soc. Expl. Geophys., 1981-1984 (2004).

[16] Draganov, D., C.P.A. Wapenaar, and J. Thorbecke, Passive seismic imaging in the presence of white noise sources, *The Leading Edge*, *23*, 889-892 (2004).

[17] Wapenaar, K., J. Fokkema and R. Snieder, Retrieving the Green's function in an open system by crosscorrelation: A comparison of approaches L, *JASA*, *118*, no.5, 2783-2786, doi:10.1121/1.2046847 (2005).

[18] Wapenaar, C., and J. Fokkema, Green's function representations for seismic interferometry, *Geophysics*, *71*, accepted for publication (2006).

[19] van Manen, D.-J., J. Robertsson, and A. Curtis, Modeling of wave propagation in inhomogeneous media, *Phys. Rev. Lett.*, *94*, 164301–1–4, doi:10.1103/PhysRevLett.94.164301 (2005).

[20] Wapenaar, C., G. Geels, V. Budejicky, and A. Berkhout, Inverse extrapolation of primary seismic waves, *Geophysics*, *54*, 853–863 (1989).